Research Article | Vol. 33, No. 5 / 10 Mar 2025 / *Optics Express* 9847

Optics EXPRESS

Generation of stable 172 nJ, 95 fs pulses from a cavity-dumped direct-diode pumped Ti:sapphire laser

SU YOUN KIM,[1,2] HONG-SEOK SEO,[1,3] HYUNGWOO KIM,[1] DO-KYEONG KO,[2,†,*] AND DONG HOON SONG[1,3,4,5,†]

[1] *R&D Center, Blue Tile Lab., 34129 Daejeon, Republic of Korea*
[2] *Department of Physics and Photon Science, Gwangju Institute of Science and Technology, Gwangju 61005, Republic of Korea*
[3] *Digital Biomedical Research Division, Digital Convergence Research Laboratory, Electronics and Telecommunications Research Institute, Daejeon 34129, Republic of Korea*
[4] *dhsong@etri.re.kr*
[5] *donghoon.song@bluetilelab.com*
[†] These authors contributed equally to this work.
[*] *dkko@gist.ac.kr*

Abstract: We demonstrate a diode-pumped Ti:sapphire laser capable of producing high-energy femtosecond pulses via cavity dumping. Four spectrally combined diodes were used to pump the Ti:sapphire laser directly, which was mode-locked using a semiconductor saturable absorber mirror. At a repetition rate of 100 kHz using a cavity dumper, 172 nJ and 95 fs pulses were generated, corresponding to a pulse peak power of 1.8 MW. The signal-to-noise ratio at the 100 kHz dumped frequency exhibited an extinction ratio exceeding 55 dB relative to the carrier. To the best of the authors' knowledge, this is the highest pulse energy obtained using a direct diode-pumped Ti:sapphire laser.

1. Introduction

Since the discovery that Ti:sapphire (Ti:S) crystals have exceptionally broad gain bandwidths, femtosecond solid-state lasers based on Ti:S crystals have become pivotal technologies across a wide spectrum of industrial and scientific applications, such as precision machining, bioimaging, ophthalmic surgery, and ultrafast science [1–7]. Conventionally, Ti:S lasers have been predominantly pumped using frequency-doubled diode-pumped solid-state lasers (DPSSLs) owing to their relatively weak absorption and short fluorescence lifetimes (3.2 μs). However, DPSSLs with inherent bulkiness are expensive and complex, limiting their widespread adoption [8,9].

The advent of high-power laser diodes (LDs) in the blue-green region has paved the way for direct diode-pumping of Ti:S crystals [10–12]. Pioneering efforts have demonstrated a blue (452 nm) diode-pumped Ti:S femtosecond laser utilizing a prism pair and a saturable Bragg reflector (SBR), generating 114 fs pulses at a 127 MHz repetition rate with 13 mW output power [13]. Subsequent work by the same group achieved an output power of 101 mW with 111 fs pulses via bidirectional pumping [14]. Concurrently, a Kerr lens mode-locked Ti:S laser pumped by two blue diodes produced 34 mW output power with 15 fs pulses [15], heralding the potential for simple, robust, and ultralow-cost Ti:S femtosecond lasers.

Recently, further advancements have led to the development of high-average-power diode-pumped Ti:S femtosecond lasers. Song *et al.* introduced an efficient approach for enhancing the mode-locked average power and pulse energy by utilizing three spectrally combined pump diodes emitting at 471, 491, and 525 nm [16]. Their setup produced self-starting femtosecond pulses with an average mode-locked power of >1 W and a 55-fs pulse duration at a 68.8 MHz repetition rate, corresponding to a pulse energy of 14.5 nJ. The same group later improved the

#554290 https://doi.org/10.1364/OE.554290
Journal © 2025 Received 27 Dec 2024; revised 12 Feb 2025; accepted 12 Feb 2025; published 25 Feb 2025

Optics EXPRESS

pulse energy to 16.3 nJ by using four diodes [17]. However, pulse energies at the 10 nJ level are still insufficient for many applications such as femtosecond laser micromachining and ultrafast nonlinear frequency conversion [18–20]. Another approach to achieving higher pulse energies involves the use of a diode-pumped regenerative amplifier system [21]. While such systems can achieve much greater pulse energies, they require additional amplification stages, resulting in increased system size, cost, and complexity. Thus, compact high-energy femtosecond lasers with high repetition rates that produce pulses with energies exceeding 100 nJ without amplification demonstrate great potential and are highly attractive because of their simplicity. The main concept is to employ an acousto-optic modulator (AOM) inside the cavity to form pulses by extracting them through cavity dumping, thereby increasing the pulse energy while maintaining the advantages of a simple and compact laser cavity. The initial successful integration of an acousto-optic cavity dumper into a Kerr lens mode-locked Ti:S laser using DPSSLs was reported by Ramaswamy *et al.* in 1993 [22]. Furthermore, the implementation of a cavity-dumped Ti:S laser using a DPSSL employing a semiconductor saturable absorber mirror (SESAM) for self-starting was demonstrated [23]. This laser produced pulse energies of up to 34 nJ at a repetition rate of 800 kHz.

In this paper, we report cavity-pumped high-energy pulses from a directly diode-pumped femtosecond Ti:S laser for the first time. An experiment was conducted to increase pulse energy and peak power with high stability. Utilizing a laser configuration based on a cavity dumper, we achieved 172 nJ pulses with durations of 95 fs in the negative dispersion regime at a repetition rate of 100 kHz, corresponding to a peak power of 1.8 MW. The mode-locked laser maintained its power with a root-mean-square (RMS) stability of 1.62% over a period exceeding 5 h. This enables the megawatt of peak power from a direct diode-pumped Ti:S laser.

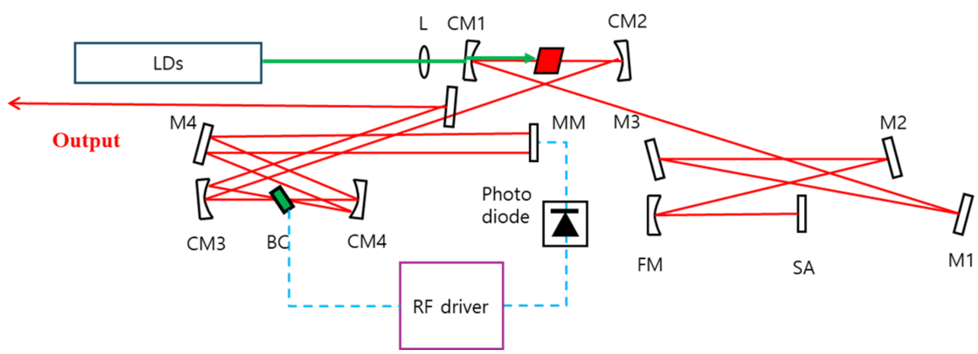

Fig. 1. Experimental setup of the cavity dumped femtosecond Ti:S laser. LDs, laser diodes; CM, dichroic curved mirror; L, lens; SA, saturable absorber; M1–M4, flat chirped mirror; MM, monitoring mirror; BC, Bragg cell; FM, Focusing mirror.

2. Experimental setup

Figure 1 illustrates the schematic configuration of the laser. The laser cavity was configured as a basic X-fold structure incorporating an AOM. The pump source comprises four diodes (450, 470, 492, and 526 nm). The combined beam is described in detail elsewhere [17]. The Ti:S crystal and the four LDs were water-cooled on copper and aluminum mounts at a temperature of 14.5 °C, and the maximum output powers of each LD were set to 4.5 W, 4.5 W, 2.0 W, and 1.2 W. Concave dichroic pump mirrors (CM1 and CM2) with a curvature radius of 100 mm were aligned at a folded angle of approximately 13° to compensate for the Ti:S crystal astigmatism. A Brewster-cut 6 mm Ti:S crystal with an absorption coefficient of 2.71 cm^{-1} at 532 nm was placed between CM1 and CM2. The cavity length is 1875 mm, which corresponds to a fundamental

Optics EXPRESS

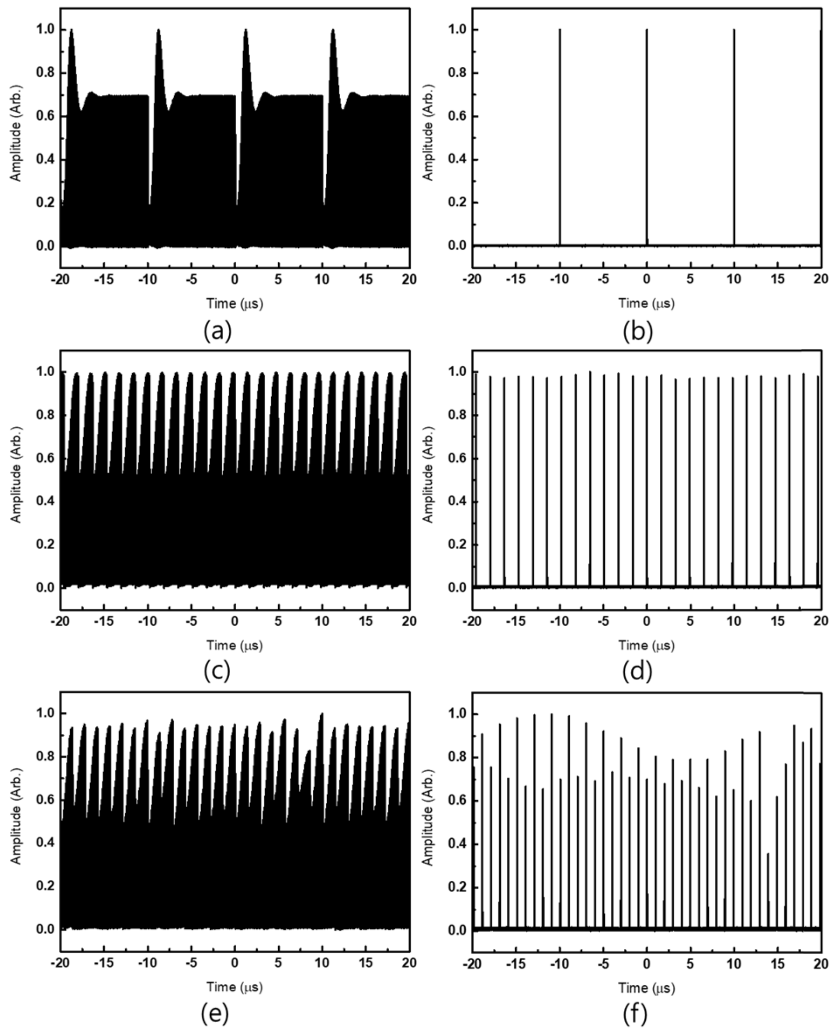

Fig. 2. States with cavity dumping and cavity-dumped pulse trains. (a) and (b) correspond to the relaxed state and dumped pulse train at a repetition rate of 100 kHz, respectively. (c) and (d) correspond to the intermediate state and dumped pulse train at a repetition rate of 612 kHz, respectively. (e) and (f) correspond to the transient state and dumped pulse train at a repetition rate of 698 kHz, respectively

repetition rate of 80 MHz. In the long arm of the cavity (CM1 to SA) at a length of 1080 mm, three planar chirped mirrors (M1, M2, and M3) were placed to generate a negative group-delay dispersion (GDD). A SESAM (labeled SA), supplied by RefleKron, was employed to initiate mode locking and placed before a concave mirror (FM) with a curvature radius of 300 mm.

The ABCD matrix was calculated to determine the beam waist within the cavity from the SESAM to the monitoring mirror (MM). The beam waists at the Ti:S gain medium and SESAM were designed to have radii of 38 μm and 250 μm, respectively. The pump mode radius in the Ti:S crystal was measured to be 39 μm. The fluence on the SESAM at a 100 kHz dumping rate was 132 $\mu J/cm^2$ with intra-cavity pulse energy of about 260 nJ, which is two times higher than the saturation fluence of 60 $\mu J/cm^2$. In the short arm (CM2 to MM) with a length of 690 mm, concave mirrors (CM3 and CM4) with a curvature radius of 150 mm were positioned to focus

Optics EXPRESS

Table 1. Summary of the cavity dumped pulse energy and stability results from the diode-pumped femtosecond Ti:S laser

States	Dumped frequency (kHz)	Ratio	Power (mW)	Pulse energy (nJ)	Pulse-to-pulse stability (RMS, %)
Relaxed	1	79580	0.171	171	0.77
Relaxed	10	7958	1.74	174	1.58
Relaxed	20	3978	3.45	172	1.24
Relaxed	50	1591	8.50	170	0.79
Relaxed	100	796	17.2	172	0.74
Relaxed	200	398	34.0	172	1.39
Intermediate	500.5	159	88.9	178	6.10
Intermediate	612	130	115	188	13.4
Transient	698	114	109	156	10.8
Transient	1000	79	114	144	6.45

the beam onto a Bragg cell (APE Berlin) aligned at the Brewster's angle. The cavity pulses were monitored using a fast photodiode to detect the leakage from the MM ($R = 99.9\%$). The cavity dumper was driven by a high-speed RF driver from the APE Berlin cavity dumper kit, which was synchronized with pulses circulating inside the cavity through signals detected from the MM output using a fast photodetector.

The RF-driven cavity dumper setup is similar to previously reported experimental configurations [22,24,25], which incorporate an additional flat-end mirror. In this arrangement, the acousto-optic cavity dumper consists solely of two concave mirrors, CM3 and CM4. The system includes a fused-silica cell positioned at Brewster's angle within the focal region of CM3. The cavity dumper exhibits a single-pass diffraction efficiency of approximately 50%. By employing a double-pass cavity-dumping technique to lead to constructive interference between the first diffracted dumped pulses and the second (returning pulses), the laser significantly improved the extraction efficiency up to 70%. Thus, this approach allows the pulse to interact with the acousto-optic Bragg cell twice, thereby enhancing the overall energy extraction and requiring more precise control over the pulse output through an optimized phase alignment. By matching the RF frequency to the laser repetition rate and optimizing the phase, the preceding and trailing pulses can be effectively suppressed, thereby ensuring accurate single-pulse extraction. To ensure the proper operation of the RF driver as well as to increase further intracavity pulse energy, the 99.9% reflective MM was utilized. The total intra-cavity GDD of approximately $-900\ \mathrm{fs}^2$ was maintained to obtain stable SESAM mode-locking [9,26].

3. Results and discussion

In general, at high dumping efficiencies, a large number of photons are suddenly extracted from the cavity, resulting in a sharp decrease in the photon number. After relaxation oscillation in the gain medium, the pulse experiences overshoot during recovery to the steady state. The dynamic behavior can be classified into distinct states such as "relaxed," "intermediate," and "transient" regimes depending on repetition rates, which is described in detail in [27]. The three distinct experimental states and corresponding dumped pulse energy with respect to the cavity dumping mode-locking at different repetition rates (dumped frequency = fundamental frequency/ratio) from 1 kHz to 1 MHz are classified and summarized in Table 1. The fundamental frequency was 79.8 MHz. At low repetition rates, that is, relaxed state as shown in Fig. 2(a), the intra-cavity pulses were sufficiently restored before being next-dumped after relaxation oscillation, resulting in stable pulse-to-pulse stability. The pulse-to-pulse stability over 1 h was measured using a

Optics EXPRESS

high-bandwidth oscilloscope (Teledyne Lecroy, WaveRunner 610Zi, 1 GHz bandwidth). At 100 kHz repetition rate as shown in Fig. 2(b), the best pulse-to-pulse stability was measured up to 0.74% RMS. The corresponding pulse energy (equivalent to the power divided by the dumped frequency) is 172 nJ. The average output power at this repetition rate and the highest pump powers of the LDs was measured to be 17.2 mW, with an optical conversion efficiency below 1%, which is characteristic of cavity-dumped lasers where intracavity pulse energy is directly extracted at the dumping frequency. This energy level and stability make the system suitable for applications requiring high pulse energy and stable operation. In intermediate states such as the 500.5 kHz and 612 kHz repetition rates, cavity dumping occurred during the relaxation oscillation process, resulting in unstable pulse-to-pulse stability as shown in Fig. 2(c) and (d). Thus, the pulse-to-pulse stabilities were 6.1% and 13.4% RMS, respectively. Although the pulse-to-pulse stability increased to three times that of the relaxed state, the highest pulse energy of 188 nJ at a repetition rate of 612 kHz was achieved. At transient states such as 698 kHz and 1 MHz repetition rate, the pulse-to-pulse stability was 10.8% and 6.45% RMS and pulse energy was 156 nJ and 144 nJ, respectively, because the intracavity pulses had insufficient time to relax oscillation before the next dumping as shown in Fig. 2(e) and (f).

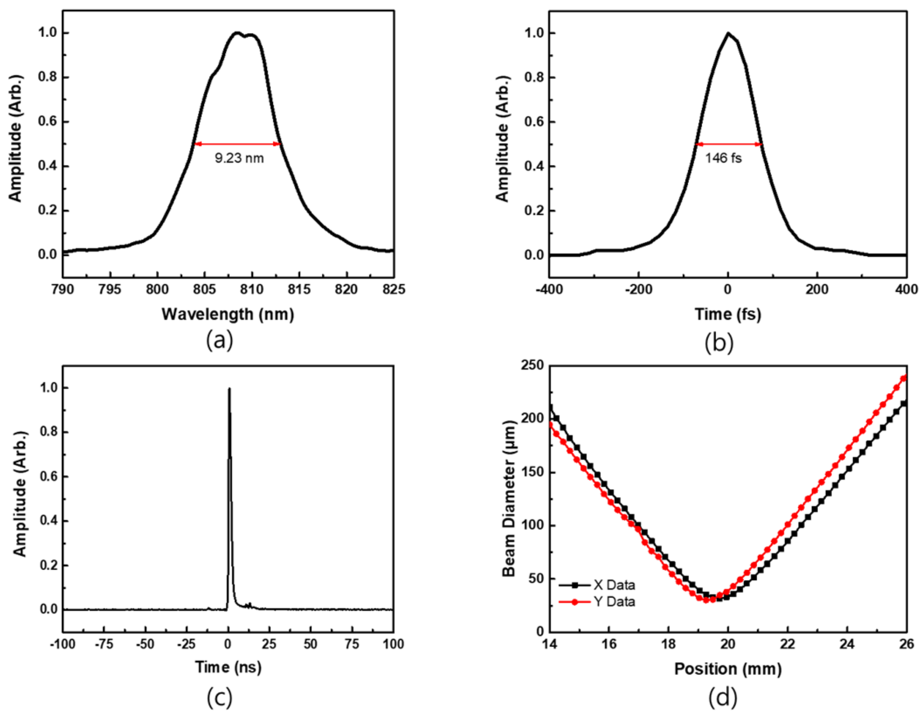

Fig. 3. (a) Measured pulse spectrum, (b) corresponding intensity autocorrelation, (c) extracted single pulse train with neighboring pulses, and (d) beam propagation factor (M^2) value.

To characterize the laser output at a 100 kHz dumped frequency, the mode-locked output spectrum, pulse width, output pulse train, and beam propagation factor M^2 were measured, as shown in Fig. 3. The spectrum in Fig. 3(a) exhibited a full width at half maximum (FWHM) of 8.23 nm centered at 808 nm, with no observable changes during laser operation. The pulse width was measured using a commercial autocorrelator (APE GmbH), yielding a FWHM autocorrelation trace of 146 fs (Fig. 3(b)), corresponding to a pulse duration of 95 fs assuming a sech^2 pulse shape. By carefully adjusting the position and angle of the AOM and precisely controlling the

Optics EXPRESS

phase and delay parameters of the RF driver, we achieved a contrast ratio exceeding 20:1 with respect to neighboring pulses. To further characterize the laser beam quality, we measured the beam propagation factor M^2 using a WinCamD-LCM beam profiler (DataRay Inc.). As shown in Fig. 3(d), the M^2 value was 1.07×1.19, indicating a slight beam astigmatism owing to the asymmetry in the optical cavity design and the different focusing positions of laser diodes with varying wavelengths.

Finally, to verify that the laser generated stable femtosecond pulses, we measured the long-term power stability and the RF spectrum. As shown in Fig. 4(a), the RMS stability of the mode-locked output power at a 100 kHz repetition rate was 1.69% over 5 h. The RF spectra of the mode-locked pulses were recorded at the fundamental frequency using a spectrum analyzer (Teledyne Lecroy, T3SA3200). Figure 4(b) shows the RF spectrum with a resolution bandwidth of 30 Hz over a span of 50 kHz. A signal-to-noise ratio of >55 dB was measured.

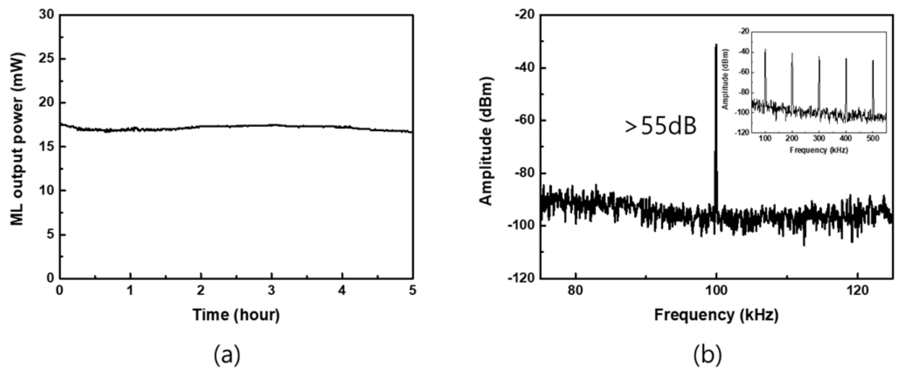

Fig. 4. (a) Mode-locked output power stability over 5 h. (b) RF spectrum at the 100 kHz dumped frequency with a resolution bandwidth of 30 Hz (inset: RF spectrum spanning 500 kHz with a resolution bandwidth of 1 kHz).

4. Conclusion

In this study, we generated a pulse energy of up to 172 nJ in a direct diode-pumped Ti:S laser using cavity dumping. By utilizing four spectrally combined diodes to directly pump the Ti:S laser employing SESAM for mode locking, femtosecond pulses with a duration of 95 fs at a repetition rate of 100 kHz were achieved. To the best of our knowledge, this is the highest pulse energy obtained using a direct diode-pumped Ti:S laser. The pulses with pulse-to-pulse stability of 0.74% RMS was not only stabilized, but power was also maintained with RMS stability of 1.69%. The signal-to-noise ratio exhibited an extinction ratio exceeding 55 dB relative to the carrier at the 100 kHz dumped frequency, indicating stable mode-locked pulses without multiple pulsing instabilities due to the Kerr nonlinearity of the gain medium.

These results demonstrate the feasibility of achieving megawatt-level peak powers in diode-pumped Ti:S lasers using the cavity-dumping technique. The combination of a high pulse energy, short pulse duration, and stable operation renders this laser suitable for ultrafast applications, such as femtosecond laser micromachining and ultrafast nonlinear frequency conversion, both of which require megawatt peak powers.

Funding. Korea Innovation Foundation (INNOPOLIS, 2023-DD-RD-0051-02); Technology Development. Program of MSS (RS-2023-00285270); Promoting Commercialization of ETRI R&D Results (25ZV1100).

Disclosures. The authors declare no conflicts of interest.

Data availability. The data underlying the results presented in this paper are not publicly available but may be obtained from the corresponding author upon reasonable request.

Optics EXPRESS

References

1. J. Klein and J. D. Kafka, "The Ti:sapphire laser: The flexible research tool," Nat. Photonics **4**(5), 289 (2010).
2. W. Drexler, U. Morgner, R. K. Ghanta, *et al.*, "Ultrahigh-resolution ophthalmic optical coherence tomography," Nat. Med. **7**(4), 502–507 (2001).
3. W. Sibbett, A. A. Lagatsky, and C. T. A. Brown, "The development and application of femtosecond laser systems," Opt. Express **20**(7), 6989–7001 (2012).
4. W. Denk, J. H. Strickler, and W. W. Webb, "Two-photon laser scanning fluorescence microscopy," Science **248**(4951), 73–76 (1990).
5. J. Cheng, A. Volkmer, L. D. Book, *et al.*, "Multiplex coherent anti-stokes Raman scattering microspectroscopy and study of lipid vesicles," J. Phys. Chem. B **106**(34), 8493–8498 (2002).
6. H. K. Soong and J. B. Malta, "Femtosecond lasers in ophthalmology," Am. J. Ophthalmol. **147**(2), 189–197.e2 (2009).
7. J. Doussot, G. Karras, F. Billard, *et al.*, "Resonantly enhanced filamentation in gases," Optica **4**(7), 764–769 (2017).
8. T. Südmeyer, S. V. Marchese, S. Hashimoto, *et al.*, "Femtosecond laser oscillators for high-field science," Nat. Photonics **2**(10), 599–604 (2008).
9. D. H. Song, W. B. Cho, H. W. Lee, *et al.*, "A compact kerr-lens mode-locked ti:sapphire oscillator with 330 nj soliton-like pulses," Laser Phys. Lett. **10**(6), 065003 (2013).
10. S. Nakamura, M. Senoh, S. Nagahama, *et al.*, "InGaN-based multi-quantum-well-structure laser diodes," Jpn. J. Appl. Phys. **35**(1B), L74–L76 (1996).
11. S. Nakamura, M. Senoh, S. I. Nagahama, *et al.*, "Blue InGaN-based laser diodes with an emission wavelength of 450 nm," Appl. Phys. Lett. **76**(1), 22–24 (2000).
12. S. Masui, T. Miyoshi, T. Yanamoto, *et al.*, "Blue and Green Laser Diodes for Large Laser Display," in *Conference on Lasers and Electro-Optics Pacific Rim* (Optica Publishing Group, 2013), paper SA1_3.
13. P. W. Roth, A. J. Maclean, D. Burns, *et al.*, "Direct diode-laser pumping of a mode-locked ti:sapphire laser," Opt. Lett. **36**(2), 304–306 (2011).
14. P. W. Roth, D. Burns, and A. J. Kemp, "Power scaling of a directly diode-laser-pumped ti:sapphire laser," Opt. Express **20**(18), 20629–20634 (2012).
15. C. G. Durfee, T. Storz, J. Garlick, *et al.*, "Direct diode-pumped kerr-lens mode-locked ti:sapphire laser," Opt. Express **20**(13), 13677–13683 (2012).
16. D. H. Song and H.-S. Seo, "Spectrally combined three-diode-pumped compact femtosecond Ti:sapphire laser exceeding 1 W mode-locked power," Opt. Express **29**(20), 32649–32657 (2021).
17. D. H. Song, C. Huh, and H.-S. Seo, "Spectrally combined four-diode-pumped femtosecond Ti:sapphire laser with 16.3 nJ pulse and its application to video-rate coherent anti-Stokes Raman scattering Spectro-Microscopy," Opt. Express **31**(2), 3269–3277 (2023).
18. A. M. Kowalevicz, V. Sharma, E. P. Ippen, *et al.*, "Three-dimensional photonic devices fabricated in glass by use of a femtosecond laser oscillator," Opt. Lett. **30**(9), 1060–1062 (2005).
19. A. Killi, A. Steinmann, G. Palmer, *et al.*, "Megahertz optical parametric amplifier pumped by a femtosecond oscillator," Opt. Lett. **31**(1), 125–127 (2006).
20. R. R. Gattass and E. Mazur, "Femtosecond laser micromachining in transparent materials," Nat. Photonics **2**(4), 219–225 (2008).
21. S. Backus, M. Kirchner, R. Lemons, *et al.*, "Direct diode pumped Ti:sapphire ultrafast regenerative amplifier system," Opt. Express **25**(4), 3666–3674 (2017).
22. M. Ramaswamy, M. Ulman, J. Paye, *et al.*, "Cavity-dumped femtosecond Kerr-lens mode-locked Ti:Al_2O_3 laser," Opt. Lett. **18**(21), 1822–1824 (1993).
23. S. Schneider, A. Stockmann, and W. Schuesslbauer, "Self-starting mode-locked cavity-dumped femtosecond Ti:sapphire laser employing a semiconductor saturable absorber mirror," Opt. Express **6**(11), 220–226 (2000).
24. M. S. Pshenichnikov, W. P. de Boeij, and D. A. Wiersma, "Generation of 13-fs. 5-MW pulses from a cavity-dumped Ti:sapphire laser," Opt. Lett. **19**(8), 572–574 (1994).
25. Y.-H. Liau, A. N. Unterreiner, D. C. Arnett, *et al.*, "Femtosecond-pulse cavity-dumped solid-state oscillator design and application to ultrafast microscopy," Appl. Opt. **38**(36), 7386–7392 (1999).
26. D. H. Song, S. I. Hwang, and D. K. Ko, "Dynamics of sub-microjoule femtosecond pulse formation in a negative dispersion regime," J. Korean Phys. Soc. **61**(5), 730–734 (2012).
27. A. Killi and U. Morgner, "Solitary pulse shaping dynamics in cavity-dumped laser oscillators," Opt. Express **12**(15), 3397–3407 (2004).